14 October 2024 15:41:13

RESEARCH ARTICLE | OCTOBER 11 2024

# Effect of post-deposition annealing on crystal structure of RF magnetron sputtered germanium dioxide thin films *⊙*

Ahmad Matar Abed ⊚ ; Rebecca L. Peterson **S** 



J. Vac. Sci. Technol. A 42, 063403 (2024)

https://doi.org/10.1116/6.0003960





## Articles You May Be Interested In

Epitaxial growth of rutile GeO<sub>2</sub> via MOCVD

Appl. Phys. Lett. (September 2024)

Insight into unusual impurity absorbability of GeO<sub>2</sub> in GeO<sub>2</sub>/Ge stacks

Appl. Phys. Lett. (October 2011)

Establishment of a growth route of crystallized rutile  $GeO_2$  thin film ( $\ge 1 \mu m/h$ ) and its structural properties

Appl. Phys. Lett. (August 2021)





# Effect of post-deposition annealing on crystal structure of RF magnetron sputtered germanium dioxide thin films

Cite as: J. Vac. Sci. Technol. A 42, 063403 (2024); doi: 10.1116/6.0003960 Submitted: 6 August 2024 · Accepted: 23 September 2024 · Published Online: 11 October 2024









Ahmad Matar Abed¹ 📵 and Rebecca L. Peterson¹.2,a) 📵



#### **AFFILIATIONS**

- <sup>1</sup>Materials Science and Engineering Department, University of Michigan, Ann Arbor, Michigan 48109
- <sup>2</sup>Electrical Engineering and Computer Science Department, University of Michigan, Ann Arbor, Michigan 48109

#### **ABSTRACT**

In this work, we demonstrate the growth and phase stabilization of ultrawide bandgap polycrystalline rutile germanium dioxide (GeO2) thin films. GeO2 thin films were deposited using RF magnetron sputtering on r-plane sapphire (Al2O3) substrates. As-deposited films were x-ray amorphous. Postdeposition annealing was performed at temperatures between 650 and 950 °C in an oxygen or nitrogen ambient. Annealing at temperatures from 750 to 950 °C resulted in mixed-phase polycrystalline films containing tetragonal (rutile)  $GeO_2$ , hexagonal ( $\alpha$ -quartz)  $GeO_2$ , and/or cubic (diamond) germanium (Ge). When nitrogen was used as the anneal ambient, mixed  $GeO_2$  phases were observed. In contrast, annealing in oxygen promoted stabilization of the r-GeO<sub>2</sub> phase. Grazing angle x-ray diffraction showed a preferred orientation of  $\frac{7}{8}$  (220) r-GeO<sub>2</sub> for all crystallized films. The combination of O<sub>2</sub> annealing and O<sub>2</sub> flux during growth resulted in r-GeO<sub>2</sub> films with highly  $\frac{2}{8}$ preferential alignment. Using electron microscopy, we observed an interfacial layer of hexagonal-oriented GeO<sub>2</sub> with epitaxial alignment to the  $(1\bar{1}02)$  Al<sub>2</sub>O<sub>3</sub> substrate, which may help stabilize the top polycrystalline r-GeO<sub>2</sub> film.

Published under an exclusive license by the AVS. https://doi.org/10.1116/6.0003960

#### I. INTRODUCTION

Ultrawide bandgap (UWBG) semiconductors are key to enabling high voltage and high power electronics as well as deep ultraviolet (UV) detectors and emitters. For instance, the UWBG oxide semiconductor β-Ga<sub>2</sub>O<sub>3</sub> is being intensively investigated due to its large breakdown field that results in a high Baliga figure of merit (BFOM), indicating its potential for high voltage power electronic devices. 1-5 However, β-Ga<sub>2</sub>O<sub>3</sub> has numerous drawbacks: it cannot be doped p-type, limiting it to unipolar device architectures, and it has a very low thermal conductivity, complicating heat extraction and thermal management. 3,6 The UWBG semiconductor germanium dioxide (GeO2) has recently gained attention as a possible alternative. 7-9 At ambient temperatures and pressures, GeO<sub>2</sub> primarily has two UWBG phases: an α-quartz-like phase (P3<sub>2</sub>21) that has a hexagonal structure and a rutile phase (P42/mnm) that has a tetragonal structure. 9-12 Recently, it has been reported that rutile germanium dioxide (r-GeO<sub>2</sub>) has a high thermal conductivity10 and is predicted to have ambipolar doping capability.7,9,13-15 These advantageous properties open the door for many potential applications in power electronic devices.

Synthesis of GeO2 is challenging because the rutile and the α-quartz-like phases have a similar free energy of formation, making it difficult to obtain a single phase material.8 It has been found previously that the glassy phase of GeO2 is the most likely phase to form at room temperature. 16 Bulk synthesis of GeO<sub>2</sub> polymorphs has previously been reported, but many of these studies have been conducted under high pressure conditions. 17,18

Thin film growth of r-GeO<sub>2</sub> has been reported using molecular beam epitaxy (MBE),8 mist chemical vapor deposition (mist CVD), 19,20 flux method, 21 pulsed laser deposition (PLD), 22-24 and metal-organic chemical vapor deposition (MOCVD).<sup>25</sup> Due to the challenge of stabilizing GeO2, various approaches have been used to obtain single crystalline rutile GeO2 films. For example, in the case of MBE, a buffer layer of SnO<sub>2</sub>/Sn<sub>x</sub>Ge<sub>1-x</sub>O<sub>2</sub> was used. For PLD and CVD, epitaxially matched substrates such as m-plane sapphire,<sup>22</sup> c-plane sapphire,<sup>23</sup> r-plane sapphire,<sup>24</sup> and rutile TiO<sub>2</sub><sup>1</sup> were used to reduce misfit strain. Physical vapor deposition (PVD)

a)Author to whom correspondence should be addressed: blpeters@umich.edu



has an advantage over CVD because it does not require the use of specialized precursor materials. Previously, by using PVD magnetron sputtering of Ge targets with an oxygen flux during deposition, nanotextured hexagonal and tetragonal cristobalite (space group P4<sub>1</sub>2<sub>1</sub>2) phases of GeO<sub>2</sub> were achieved on silicon (100) and quartz substrates. 16 In that work, Nalam et al. used a Ge target with oxygen flux during deposition, which provided limited control of oxidation during growth.

In this study, to harness PVD to achieve rutile-phase GeO2 films, we used a GeO2 target and oxygen flux during magnetron sputtering to improve control of oxygen incorporation into GeO<sub>2</sub> thin films. We used r-plane sapphire as the substrates because of its epitaxial relation with rutile structures, reported previously.<sup>8,24</sup> We investigated the effects of oxygen-to-argon flux during growth and of the ambient during postdeposition annealing (PDA) on the structural properties of GeO2 thin films and determined the conditions necessary to reduce crystallization of the hexagonal phase and promote formation of the rutile phase. We demonstrated that a combination of 1:5 O2:Ar ratio during growth followed by postdeposition anneal in O2 results in rutile polycrystalline GeO2 films with highly preferential alignment. We observed that an interfacial layer of epitaxial h-GeO<sub>2</sub> formed in situ on the sapphire substrate helps to stabilize the top polycrystalline r-GeO<sub>2</sub> film. Optical measurements were performed on the r-GeO<sub>2</sub> preferred oriented films, which confirmed the UWBG nature of the material.

#### II. EXPERIMENTAL DETAILS

To grow GeO2 thin films, we used commercially available r-plane sapphire  $10 \times 10 \text{ mm}^2$  substrates. The substrates were solvent cleaned with acetone and isopropyl alcohol in a 40 °C ultrasonic tank for 10 min each. Using RF magnetron sputtering (RFMS) in a Kurt J. Lesker PRO Line PVD 75, GeO2 was deposited on top of the substrates. A 3-in. GeO<sub>2</sub> (99.999%) target (Princeton Scientific) was used with a target to-substrate distance of  $\sim 16$  cm. All depositions used an RF power of 300 W, a process pressure of  $5 \times 10^{-3}$  Torr, a deposition time of 1200 s, and had no intentional heating or cooling of the substrate during deposition. These conditions were selected to achieve a reasonable growth rate and film thickness of approximately 100 nm through initial experiments depositing GeO2 on silicon wafers. The O2 flux during growth was varied between 0% and 30%, with the balance made up of Ar. Following thin film deposition, PDA was performed at temperatures ranging from 650 to 950 °C in either an oxygen or a nitrogen ambient. An Angstrom Engineering low pressure chemical vapor deposition furnace was used for the PDA, with a heating ramp rate of 100 °C/min. X-ray diffraction (XRD) experiments were performed using a Rigaku SmartLab diffractometer ( $\lambda = 1$ . 5406 Å). The incident angle was set to  $\omega = 0.5^{\circ}$  to maximize the peak intensity for all grazing incidence x-ray diffraction (GIXRD) measurements. To study the morphology of the films, atomic force microscopy (AFM) was performed using a Veeco Dimension Icon AFM tool.

To study the structural nature of the films, scanning transmission electron microscopy (STEM) and selected area electron diffraction (SAED) were performed on a TFS Talos F200X G2 transmission electron microscope system equipped with a SuperX energy-dispersive x-ray spectrometer (200 keV operating condition). Focused ion beam (FIB)-assisted lift-out was conducted using a TFS Helios 650 Nanolab SEM. Prior to lift-out, carbon and platinum capping layers were deposited in situ to protect the film from FIB damage. Optical spectroscopy (UV-vis) was performed using a Cary 50 Bio UV-Visible Spectrophotometer.

#### **III. RESULTS AND DISCUSSION**

The first films were deposited with no oxygen flux during sputtering. The thickness of the as-deposited film was measured by electron microscopy to be approximately 100 nm. AFM was used to measure an RMS roughness of 0.3 nm. Figure S1 in the supplementary material shows a cross-sectional high-angle annular dark-field (HAADF) image and the AFM scan of an as-deposited

The structural properties of the GeO<sub>2</sub> thin film were studied using GIXRD. Using films deposited with no oxygen flux during growth, we performed PDA in a nitrogen ambient [Fig. 1(a)]. The PDA temperature ranged from 650 to 950 °C. The as-deposited film is x-ray amorphous. Crystallization starts at annealing temperatures of 650 °C and above. The films annealed at 650, 750, 850, and 950 °C are polycrystalline with mixed phases of rutile and hexagonal GeO2, as well as Ge diamond cubic crystals. The presence of r-GeO<sub>2</sub> crystallites is a promising first step.

Next, we sought to determine whether incorporating oxygen during growth and annealing would promote rutile germanium 3 oxide formation. A second set of samples was prepared with 20% oxygen flux used during growth, and the PDA was performed in an oxygen ambient [Fig. 1(b)]. These samples are also x-ray amorphous as deposited. Crystallization begins at annealing temperatures of 750 °C and above. This is different from the films prepared  $\stackrel{\circ}{\approx}$ without oxygen flux, for which crystallization started at 650 °C. For  $\frac{12}{60}$ the samples prepared with oxygen flux during deposition and oxygen PDA at 750 and 850 °C, the films are polycrystalline with a mixed phase of rutile and hexagonal GeO2, as well as Ge diamond cubic. As the anneal temperature increases from 750 to 950 °C, we observe an increasing preference for r-GeO<sub>2</sub> with a predominant (220) orientation. We performed a similar experiment using 30% oxygen flux and found that the film grown with 20% O2 flux has a relatively stronger (220) peak and more rutile peaks (Fig. S2 in the supplementary material), and therefore, we used 20% O2 flux during growth for the remaining experiments. Thus, we conclude that by using 20% O2 flux during deposition and an O2 annealing ambient, we can obtain films that are predominantly r-GeO<sub>2</sub> with preferential (220) orientation, compared to films deposited with no oxygen flux or 30% oxygen flux during growth and annealed under N<sub>2</sub> ambient.

High-resolution 2-theta/omega XRD measurement was performed on the O<sub>2</sub> annealed 950 °C film [Fig. 2(a)]. Based on prior work, (101) r-GeO2 is the expected orientation aligned to the r-plane substrate.<sup>8,24</sup> However, this orientation was not observed in our 2-theta/omega measurements. Rather, a (100)-oriented h-GeO<sub>2</sub> component of the film was observed, oriented to the (1102) Al<sub>2</sub>O<sub>3</sub> substrate peak. Recently, Rahaman et al. reported the growth of polycrystalline GeO2 by MOCVD, in which they observed a

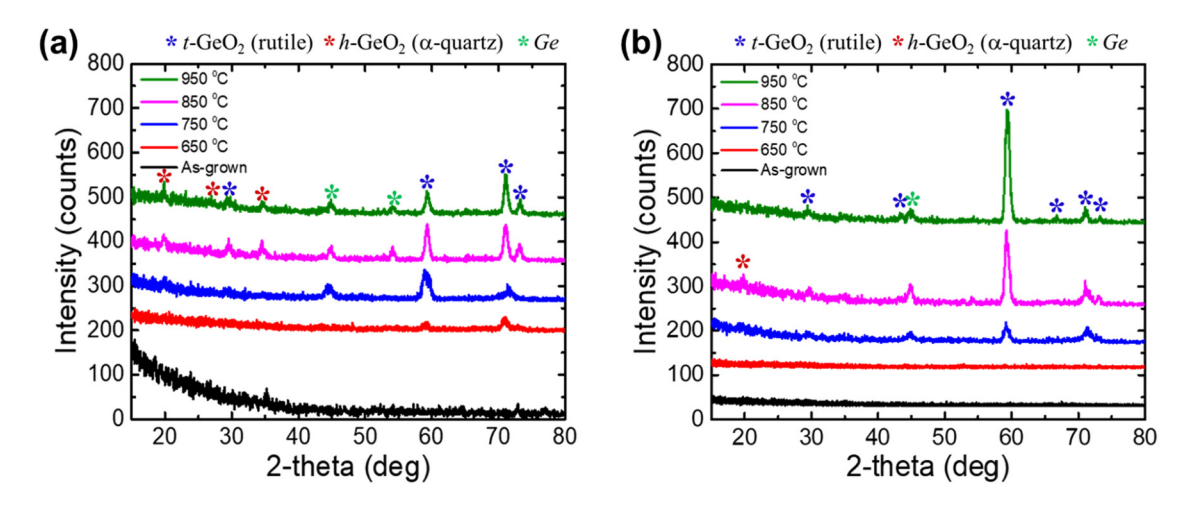


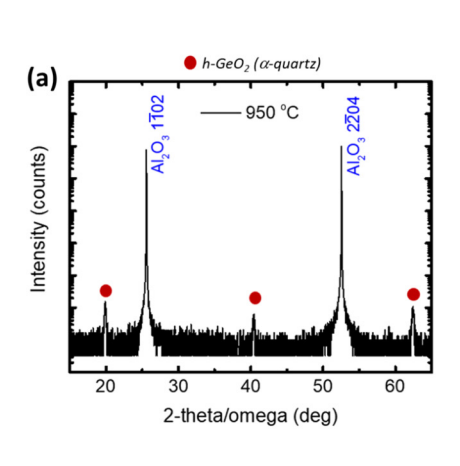
FIG. 1. Grazing incidence XRD of films deposited on r-plane sapphire with (a) no oxygen flux during growth and N2-ambient PDA; (b) oxygen flux during growth and O<sub>2</sub>-ambient PDA. The (220) r-GeO<sub>2</sub> peak is located near 60°.

polycrystalline h-GeO<sub>2</sub> phase oriented to the r-plane sapphire

By HAADF-STEM and SAED [Fig. 2(b)], we observe that the h-GeO<sub>2</sub> (100)-oriented crystals form a thin interfacial layer between the sapphire substrate and the top (220)-oriented r-GeO<sub>2</sub> polycrystalline film. The thin h-GeO<sub>2</sub> (100)-oriented layer, which is epitaxially aligned to the r-plane Al<sub>2</sub>O<sub>3</sub> substrate, may help stabilize the (220)-oriented r-GeO<sub>2</sub> polycrystalline film.

While r-GeO<sub>2</sub> polycrystalline films have been achieved, so far it is not clear whether the morphology is due to the use of O2 flux during deposition or the use of an O2 ambient during

postdeposition annealing. To investigate this, we took two samples that were grown identically with 20% O2 flux and subjected them to PDA at 950 °C. One of the samples was annealed in O2, while the other was annealed in N2. After annealing, GIXRD scans were performed on both samples. The GIXRD traces for these films are shown in Fig. 3. The sample annealed in O2 has significantly stronger r-GeO<sub>2</sub> peaks compared to the film annealed in N<sub>2</sub>. We con- $\frac{2}{3}$ clude that both O<sub>2</sub> flux during growth and O<sub>2</sub> postdeposition annealing are needed to obtain the predominant (220)-orientated r-GeO $_2$  film. We hypothesize that the use of oxygen during both  $\stackrel{\circ}{8}$ film synthesis and postdeposition annealing decreases the density



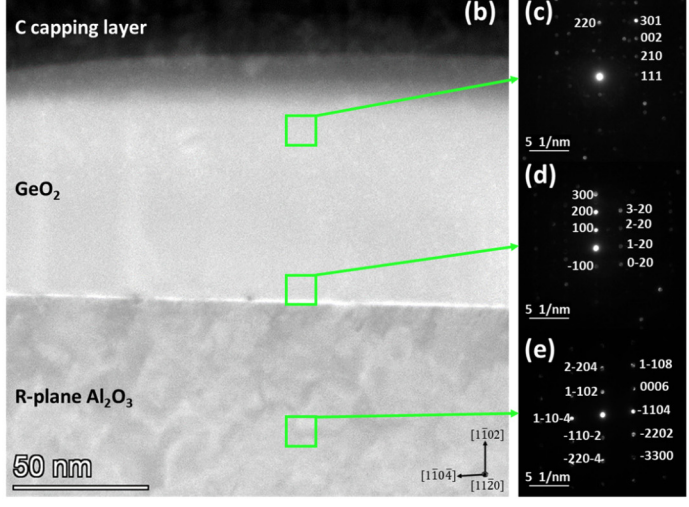
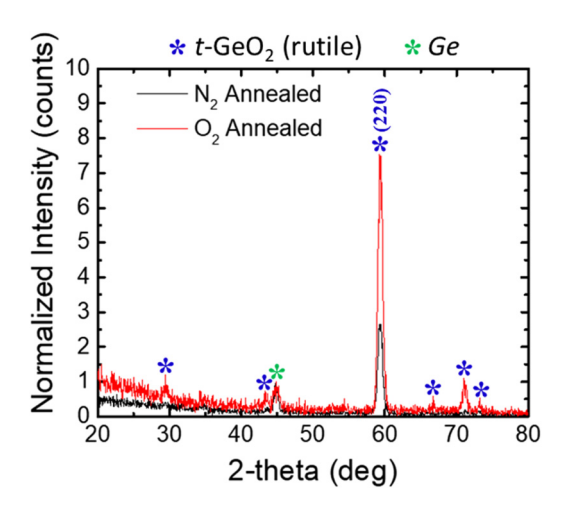


FIG. 2. Characterization of GeO2 films deposited with 20% O2 flux and annealed at 950 °C in O2. (a) High-resolution 2-theta/omega XRD showing that (100) h-GeO2 is epitaxially aligned to (1102) Al<sub>2</sub>O<sub>3</sub>. (b) HAADF STEM cross-sectional image of the GeO<sub>2</sub>/Al<sub>2</sub>O<sub>3</sub> interface and the GeO<sub>2</sub> film. (c)-(e) SAED patterns of (c) the polycrystalline GeO<sub>2</sub> film; (d) the GeO<sub>2</sub> film above the interface, showing (100) h-GeO<sub>2</sub> epitaxially aligned to (1102) Al<sub>2</sub>O<sub>3</sub>; and (e) the Al<sub>2</sub>O<sub>3</sub> substrate.





**FIG. 3.** Grazing incidence XRD results for films grown with 20% oxygen flux annealed at 950 °C using either nitrogen or oxygen as the anneal ambient. For comparison, the intensities of each trace are normalized that trace's peak value at the Ge diamond cubic peak near 45°, indicated with a green star.

of oxygen-related defects and promotes the oxidation of Ge to obtain r-GeO<sub>2</sub>.

Optical characterization of the GeO<sub>2</sub> film deposited with 20% O<sub>2</sub> flux and annealed at 950 °C in O<sub>2</sub> was performed at room temperature to correlate its structural and optical properties. The Tauc plot is shown in Fig. 4. To determine the direct bandgap, we fit the data to the equation  $(\alpha h \gamma)^2 = B(h \gamma - E_g)$ , where  $\alpha$  is the absorption coefficient,  $h \gamma$  is the photon energy, and B is a constant. The extracted bandgap is 5.1 eV, confirming the UWBG nature of the

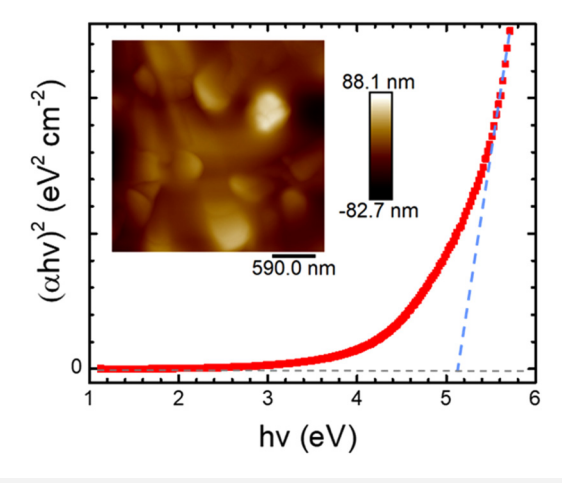


**FIG. 4.** Tauc plot based on absorption measurements of the  ${\rm GeO_2}$  film deposited with 20%  ${\rm O_2}$  flux and annealed at 950 °C in  ${\rm O_2}$ . The linear extrapolation (dashed line) indicates that the bandgap of the film is 5.1 eV. The inset shows the surface morphology of the film measured by AFM, with an RMS roughness of  $\sim\!20$  nm.

film. The obtained bandgap of the  $GeO_2$  film is wider than the reported values of 4.6 (Ref. 27) and 4.68 eV<sup>13</sup> for bulk r-GeO<sub>2</sub>. However, the 5.1 eV bandgap we measured is in agreement with recent experimental work and theoretical predictions of the first allowed optical transition on r-GeO<sub>2</sub> thin films. <sup>14,22–24</sup> This result confirms the structural analysis, which showed that our film has a polycrystalline r-GeO<sub>2</sub> morphology.

Finally, the surface roughness of morphology of the  $GeO_2$  film deposited with 20%  $O_2$  flux and annealed at 950 °C in  $O_2$  was studied using AFM. The scan is shown in the inset of Fig. 4. The RMS roughness of the film surface is approximately 20 nm.

#### IV. SUMMARY AND CONCLUSIONS

In this paper, we investigated the effects of oxygen flux during growth of GeO<sub>2</sub> thin films and of the ambient used during postdeposition anneal on the films' structural morphology. A new method to grow and phase-stabilize rutile polycrystalline GeO<sub>2</sub> films was established. For samples grown with 20% oxygen flux followed by a PDA in oxygen at temperatures ranging from 750 to 950 °C, r-GeO<sub>2</sub> with preferential (220) orientation was observed. In contrast, when nitrogen was used as the anneal ambient, a mixed GeO<sub>2</sub> phase results for all annealing temperatures studied (650-950 °C). This shows that oxygen annealing promotes the stabilization of the r-GeO<sub>2</sub> phase, and that a combination of O<sub>2</sub> annealing and O2 flux of 20% during growth results in r-GeO2 films with highly preferential alignment. From STEM of the GeO<sub>2</sub> film deposited with 20% O2 flux and annealed at 950 °C in O2, we observed that an epitaxial h-GeO<sub>2</sub> film forms in situ at the r-plane Al<sub>2</sub>O<sub>3</sub> substrate interface, which may help stabilize the top polycrystalline r-GeO2 film.

In conclusion, this study has demonstrated a new synthesis  $\frac{80}{100}$  route to achieve  $r\text{-}\text{GeO}_2$  on sapphire using PVD from  $\frac{80}{100}$  targets, 20%  $\frac{8}{100}$  flux during deposition, and postdeposition anneal in  $\frac{8}{100}$  ambient. This growth is a key step in the fabrication process of future power electronics devices based on this promising UWBG semiconductor. Future work is needed to better understand how other deposition conditions such as the fraction of oxygen flux, the substrate temperature during deposition, and the choice of substrate may affect the formation of r- and/or h-GeO $_2$ . In addition, further work is needed to understand the formation and role of the interfacial layer of h-GeO $_2$  on the r-GeO $_2$  film properties. To improve the GeO $_2$  films' crystal quality, in the future it would be interesting to investigate the effect of elevated substrate temperature during sputtering on the film phase purity and uniformity.

#### SUPPLEMENTARY MATERIAL

See the supplementary material for a cross-sectional HAADF STEM image, an AFM image of a film deposited with no oxygen flux and no subsequent PDA, and GIXRD traces for films deposited with 20% and 30%  $\rm O_2$  flux during growth and annealed at 950 °C in  $\rm O_2$  ambient.

### **ACKNOWLEDGMENTS**

This material is based upon work supported by the National Science Foundation Graduate Research Fellowship under Grant No.



DGE-1841052, NSF DMR FuSE teaming Award No. #2235208, and NSF DMR FuSE-1 Award No. #2328701. Any opinions, findings, and conclusions or recommendations expressed in this material are those of the authors and do not necessarily reflect the views of the National Science Foundation. Portions of this work were conducted in Lurie Nanofabrication Facility (LNF), Michigan Center for Materials Characterization (MC)<sup>2</sup>, and Van Vlack Lab, which are supported by the University of Michigan's College of Engineering.

#### **AUTHOR DECLARATIONS**

#### **Conflict of Interest**

The authors have no conflicts to disclose.

#### **Author Contributions**

Ahmad Matar Abed: Conceptualization (equal); Data curation (equal); Formal analysis (equal); Investigation (equal); Methodology (equal); Validation (equal); Visualization (equal); Writing – original draft (equal); Writing – review & editing (equal). Rebecca L. Peterson: Conceptualization (equal); Data curation (equal); Funding acquisition (equal); Methodology (equal); Project administration (equal); Supervision (equal); Validation (equal); Visualization (equal); Writing – original draft (equal); Writing – review & editing (equal).

#### **DATA AVAILABILITY**

The data that support the findings of this study are available from the corresponding author upon reasonable request.

#### **REFERENCES**

- <sup>1</sup>J. Y. Tsao et al., Adv. Electron. Mater. 4, 1600501 (2018).
- <sup>2</sup>M. Higashiwaki, AAPPS Bull. 32, 3 (2022).
- <sup>3</sup>A. J. Green et al., APL Mater. **10**, 029201 (2022).
- <sup>4</sup>J. Zhang, J. Shi, D.-C. Qi, L. Chen, and K. H. L. Zhang, APL Mater. **8**, 020906 (2020).

- <sup>5</sup>B. Chatterjee, K. Zeng, C. D. Nordquist, U. Singisetti, and S. Choi, IEEE Trans. Compon. Packag. Manuf. Technol. **9**, 2352 (2019).
- <sup>6</sup>S. J. Pearton, J. Yang, P. H. Cary IV, F. Ren, J. Kim, M. J. Tadjer, and M. A. Mastro, Appl. Phys. Rev. 5, 011301 (2018).
- <sup>7</sup>S. Chae et al., Appl. Phys. Lett. 118, 260501 (2021).
- <sup>8</sup>S. Chae, H. Paik, N. M. Vu, E. Kioupakis, and J. T. Heron, Appl. Phys. Lett. 117, 072105 (2020).
- <sup>9</sup>S. Chae, J. Lee, K. A. Mengle, J. T. Heron, and E. Kioupakis, Appl. Phys. Lett. 114, 102104 (2019).
- <sup>10</sup>S. Chae, K. A. Mengle, R. Lu, A. Olvera, N. Sanders, J. Lee, P. F. P. Poudeu, J. T. Heron, and E. Kioupakis, Appl. Phys. Lett. 117, 102106 (2020).
- 11 G. S. Smith and P. B. Isaacs, Acta Crystallogr. 17, 842 (1964).
- <sup>12</sup>Q.-J. Liu, Z.-T. Liu, L.-P. Feng, and H. Tian, Solid State Sci. **12**, 1748 (2010).
- <sup>13</sup>C. A. Niedermeier, K. Ide, T. Katase, H. Hosono, and T. Kamiya, J. Phys. Chem. C **124**, 25721 (2020).
- <sup>14</sup>K. A. Mengle, S. Chae, and E. Kioupakis, J. Appl. Phys. 126, 085703 (2019).
- <sup>15</sup>K. Bushick, K. A. Mengle, S. Chae, and E. Kioupakis, Appl. Phys. Lett. 117, 182104 (2020).
- <sup>16</sup>P. G. Nalam, D. Das, S. Tan, and C. V. Ramana, ACS Appl. Electron. Mater. 4, 3115 (2022).
- <sup>17</sup>V. V. Brazhkin, A. G. Lyapin, R. N. Voloshin, S. V. Popova, E. V. Tat'yanin, N. F. Borovikov, S. C. Bayliss, and A. V. Sapelkin, Phys. Rev. Lett. 90, 145503 (2003)
- <sup>18</sup>V. P. Prakapenka, G. Shen, L. S. Dubrovinsky, M. L. Rivers, and S. R. Sutton, J. Phys. Chem. Solids. **65**, 1537 (2004).
- <sup>19</sup>H. Takane and K. Kaneko, Appl. Phys. Lett. **119**, 062104 (2021).
- <sup>20</sup>H. Takane, Y. Ota, T. Wakamatsu, T. Araki, K. Tanaka, and K. Kaneko, Phys. Rev. Mater. 6, 084604 (2022).
- <sup>21</sup>S. Chae et al., J. Vac. Sci. Technol. A 40, 050401 (2022).
- <sup>22</sup>G. Deng, K. Saito, T. Tanaka, M. Arita, and Q. Guo, Appl. Phys. Lett. 119, 182101 (2021)
- <sup>23</sup>G. Deng, Y. Huang, Z. Chen, K. Saito, T. Tanaka, M. Arita, and Q. Guo, Mater. Lett. 326, 132945 (2022).
- <sup>24</sup>G. Deng, Y. Huang, Z. Chen, K. Saito, T. Tanaka, M. Arita, and Q. Guo, J. Luminescence 267, 120353 (2024).
- <sup>25</sup>I. Rahaman, B. Duersch, H. D. Ellis, M. A. Scarpulla, and K. Fu, arXiv:2407. 02682 (2024).
- 26I. Rahaman, H. D. Ellis, K. Anderson, M. A. Scarpulla, and K. Fu, ACS Appl. ω Eng. Mater. 2, 1724 (2024).
- <sup>27</sup>M. Stapelbroek and B. D. Evans, Solid State Commun. 25, 959 (1978).